ELSEVIER

NDT&E International 32 (1999) 225–234

NDT&E international

Modeling elastic wave propagation in waveguides with the finite element method

Friedrich Moser[a,1], Laurence J. Jacobs[a,*], Jianmin Qu[b]

[a]*School of Civil and Environmental Engineering, Georgia Institute of Technology, Atlanta, GA 30332, USA*
[b]*G. W. Woodruff School of Mechanical Engineering, Georgia Institute of Technology, Atlanta, GA 30332, USA*

Received 28 February 1998; received in revised form 24 May 1998; accepted 8 June 1998

Abstract

This paper reports on the application of guided waves techniques to nondestructively determine the structural integrity of engineering components. Specifically, this research uses a commercial finite element (FE) code to study the propagation characteristics of ultrasonic waves in annular structures. In order to demonstrate the accuracy of the proposed FE technique, the propagation of guided waves in a flat plate is examined first. Next, the propagation of guided waves in thick ring structures is investigated. Finally, these FE results are compared to analytical and experimental results. The results of this study clearly illustrate the effectiveness of using the FE method to model guided wave propagation problems and demonstrate the potential of the FE method for problems when an analytical solution is not possible because of ''complicated'' component geometry.

Keywords: Finite element method; Annular structures; Guided waves

1. Introduction

Conventional ultrasonic methods, such as pulse-echo, have been used successfully to interrogate structural components. However, the application of these traditional techniques has been limited to testing relatively simple geometries or interrogating the region in the immediate vicinity of the transducer. A new, more promising ultrasonic methodology uses guided waves to examine structural components. The advantages of this technique include: its ability to test the entire structure in a single measurement; and its capacity to test inaccessible regions of complex components.

In general, a guided wave consists of many different modes that propagate independently through the structure. The wave propagation phenomena (waveform) that is measured consists of the superposition of all of these modes. These waves interact with defects, and with geometrical features such as corners and curved surfaces, causing reflections and mode conversion. Clearly, the propagation of guided waves in a complex structure is a complicated process that is difficult to understand and interpret. The current research develops the mechanics fundamentals that models this propagation; this work is the required first step needed to develop a nondestructive evaluation technique to harness guided waves to interrogate a structural component.

One approach to modeling guided wave propagation phenomena is to analytically solve the governing differential equations of motion and their associated boundary conditions. This procedure can be (and already has been) done for ''easy'' geometries and perfect specimens (no defects). Analytical guided wave models are available for plates in Refs [1,2], or more recently for an annulus in Ref. [3]. However, these equations become intractable for more complicated geometries or for a non-perfect specimen. Another approach to this problem is a numerical solution; the main advantage of this approach is that the difficulties associated with ''complicated'' geometries and defects are much easier to handle numerically. There are basically two numerical methods which can be used for this problem: the finite element (FE) method or the boundary element (BE) method. The BE method has the advantage that just the surface of the specimen needs to be discretized; the numerical problem itself is therefore reduced by one dimension. On the other hand, the primary advantage of the FE method is that there are numerous commercial FE codes available, thus eliminating any need to develop actual code. These commercial FE codes have the additional advantages of being very user friendly, and providing sophisticated pre- and post-processing options. In addition, previous

* Corresponding author. Tel: +1-404-894-2771; fax: +1-404-894-0211.
E-mail address: laurence.jacobs@ce.gatech.edu (L.J. Jacobs)
[1] Present address: Institute A of Mechanics, University of Stuttgart, Pfaffenwaldring 9, 70550 Stuttgart, Germany.

0963-8695/99/$ – see front matter
PII: S0963-8695(98)00045-0

researchers [4] used the FE method to numerically calculate dispersion curves in a plate, clearly demonstrating that it is possible to use the FE method for guided wave propagation problems.

In order to be pertinent for nondestructive testing purposes, the FE models developed in this research must be able to accurately represent ultrasonic waves with frequencies in the MHz range. These high frequencies require a high time resolution (small time increments between calculated solution points), even for very short real times (μs range). In addition, these MHz frequencies have very short wavelengths, so the numerical model must have small element lengths to accurately resolve these spatial features; this high spatial resolution requires very small elements, in the mm range or below. An additional complication of this small element size is that a large number of elements (and thus a large system of equations) is needed to model a realistic component. As a result, the FE solution requires the inversion of a large stiffness matrix, leading to a requirement for significant computational power.

The objective of this research is to compare known (analytical) solutions of guided wave propagation problems with numerically obtained solutions. This is done in order to establish the validity of using the FE method to model annular wave guides. Two different geometries are studied: first, the well known plate, using a full transient approach to develop dispersion curves for the first few modes; and second, an annular ring for which an analytical solution was recently developed [3]. The results of both of these geometries are used to develop and test guidelines for the application of commercial FE codes for guided wave problems of more complicated geometries. As a final check, the FE results from the ring are validated with the results from an experimental procedure that uses laser ultrasonic techniques.

It is important to note that this work uses a commercial, general-purpose FE code. The advantage of a commercial code is that they are readily available in most mechanics research groups, so no extra investment is necessary. However, these general-purpose FE codes lack certain features (such as energy absorbing elements) that are available in specialized wave propagation codes. As a result, a secondary aim of this work is to find out the accuracy that can be reached with a non-specialized, general-purpose FE program. The FE program used in this work is Ansys 5.3, the research version which is limited to 64 000 nodes. However, these results are generic in nature and are relevant for any large scale commercial FE code.

2. Application of the finite element method

This research is based on the assumptions of linear elasticity. The general equations of motion in matrix form are given as:

$$\mathbf{M}\ddot{\boldsymbol{u}} + \mathbf{C}\dot{\boldsymbol{u}} + \mathbf{K}\boldsymbol{u} = \boldsymbol{F}_{\mathrm{a}}, \tag{1}$$

where **M** is the structural mass matrix; **C** is the structural damping matrix; **K** is the structural stiffness matrix; $\boldsymbol{F}_{\mathrm{a}}$, is the vector of applied loads; and u, $\dot{\boldsymbol{u}}$, and $\ddot{\boldsymbol{u}}$ are the displacement vector and its time derivatives, respectively. Damping is not considered in this study. Eq. (1) is solved using the Newmark time integration method[5].

Temporal and spatial resolution of the finite element model is critical for the convergence of these numerical results. The integration time step, Δt, is the step size for which Eq. (1) is solved. Choosing an adequate integration time step, Δt, is very important for the accuracy of the solution. In general, the accuracy of the model can be increased with increasingly smaller integration time steps. With time steps that are too long, the high frequency components are not resolved accurately enough. On the other hand, too small time steps are a waste of calculation time. Therefore, a compromise must be found. For the Newmark time integration scheme, this compromise is 20 points per cycle of the highest frequency results; this gives accurate solutions in an efficient manner [6]. This rule is expressed as:

$$\Delta t = \frac{1}{20 f_{\max}} \tag{2}$$

where $f_{\max}$ is the highest frequency of interest. By determining the highest frequency for waves propagating through the structure, and using Eq. (2), a time step, Δt, is calculated that is small enough to model the temporal behavior of the propagation. If the input function gets close to a step function, the ratio given in Eq. (2) might not provide sufficient temporal resolution. In some cases, this ratio has to be increased up to $\Delta t = (1)/(180 f_{\max})$ [6]. Also, the needed time step can alternatively be related to the time the fastest possible wave needs to propagate between successive nodes in the mesh.

This research uses two-dimensional (2D) solid structural elements that model plane strain in the z-direction. These elements are defined by four nodes with 2 degrees-of-freedom at each node: translations in the x- and y-directions. In order to mesh non-rectangular areas with elements of similar size, a few triangular shaped elements are needed; these elements are taken as degenerated quadrilateral elements. The mass distribution of all the elements is uniform. The size of the elements are chosen in a manner so that the propagating waves are spatially resolved. In Ref. [4], it is recommended that more than 10 nodes per wavelength be used, while in Ref. [6], the recommendation is much higher (on the order of 20 nodes per wavelength). The recommendation of Ref. [6] can be expressed as:

$$l_{\mathrm{e}} = \frac{\lambda_{\min}}{20} \tag{3}$$

where l_{e} is the element length and $\lambda_{\min}$ is the shortest

Table 1
FE models

Model I: Plate				
Thickness	Length	Element length	Elements	Nodes
$2b = 2$ mm	$l = 100$ mm	$l_e = 0.1$ mm	20 000	21 021
Model II: Ring				
Inner radius	Outer radius	Element length	Elements	Nodes
$r_i = 51.05$ mm	$r_o = 63.15$ mm	$l_e = 0.3$ mm	26 950	27 571

Table 2
Material properties

Material I: Plate		
Young's modulus	Poisson's ratio	Density
$E = 200\ 10^3$ N/mm^2	$\nu = 0.29$	$\rho_0 = 7850$ kg/m^3
Compression wave	Shear wave	Rayleigh wave
$c_1 = 5778$ m/s	$c_2 = 3142$ m/s	$c_R = 2909$ m/s
Material II: Ring structure		
Young's modulus	Poisson's ratio	Density
$E = 200 \times 10^3$ N/mm^2	$\nu = 0.2818$	$\rho_0 = 8030$ kg/m^3
Compression wave	Shear wave	Rayleigh wave
$c_1 = 5660$ m/s	$c_2 = 3120$ m/s	$c_R = 2886$ m/s

wavelength of interest. Similar to the process for determining the integration time step, Δt, the range of interest with respect to wavelength, λ, must first be set. If highly accurate numerical results are needed (for prediction of amplitude attenuation or precise modeling of dispersion effects), Eq. (3) might not be sufficient, and a higher level of discretization might be required.

Eqs. (2) and (3) show that for high frequency wave propagation problems, enormous computer resources are needed. Computing such problems leads to high values of f_{max}, and also small values of λ, which means a very dense mesh and very small integration time steps. As an example of the order of such a problem, consider the solution for frequencies up to $f_{max} = 2$ MHz and wavelength as low as $\lambda_{min} = 2$ mm. The solution to this problem requires an integration time step $\Delta t = 0.025$ μs and an element length $l_e = 0.1$ mm. As a result, the FE model of a 10 cm long and 1 cm thick plate requires 100 000 elements. Note that the size of the matrix equation is of the order of twice the number of elements (each node has 2 degrees-of-freedom) and that this large matrix equation must be solved for every $\Delta t = 0.025$ μs, which means that for a real time of 50 μs 2000 solution steps must be calculated. For nondestructive testing applications, this example size is very realistic and is definitely not at the upper limit of the frequency content measured in experimental models.

3. Numerical results and discussion

In order to understand the behavior and robustness of the FE method applied to the solution of guided wave problems, a relatively simple geometry is considered first: a 2 mm thick and 100 mm long steel plate. This geometry has the advantage of a known analytical solution (the Rayleigh–Lamb equation) in the form:

$$F(\alpha,\beta,\xi) = \frac{\tan\beta b}{\tan\alpha b} + \left\{\frac{4\alpha\beta\xi^2}{(\xi^2-\beta^2)^2}\right\}^{\pm 1} = 0 \qquad (4)$$

$$\begin{cases} +1 & = \text{symmetric mode} \\ -1 & = \text{antisymmetric mode,} \end{cases}$$

where α and β are parameters depending on the wave frequency, the wavenumber and the wave velocity [1]. The FE model formulated to solve this configuration is summarized in Table 1 as Model I. The material properties and the resulting wave speeds are given in Table 2 as Material I. The upper left corner of this plate, which is modeled with square shaped elements ($l_e = 0.1$ mm), is loaded with a displacement boundary condition in the x- and y-directions. Fig. 1(a) shows the applied displacements on the different nodes in the upper left corner of the plate, and Fig. 1(b) shows the time function of these displacements. This load has no practical meaning, but its frequency content is appropriate for exciting high frequency waves. The goal of this model is to show dispersion effects up to a frequency, f, of 5 MHz. According to the recommendations in the previous section, this transient problem is solved with a integration time step, $\Delta t = 10^{-8}$ s. Fig. 2 shows the x displacement of a typical node at the upper surface of the plate. In order to get dispersion curves out of this data, a 2D Fast Fourier Transformation (2D-FFT) is performed [4,7].

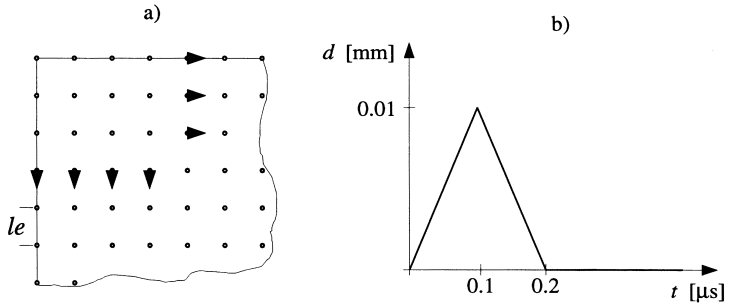

Fig. 1. Transient excitation of several modes in a plate: displacement direction and time function of applied load.

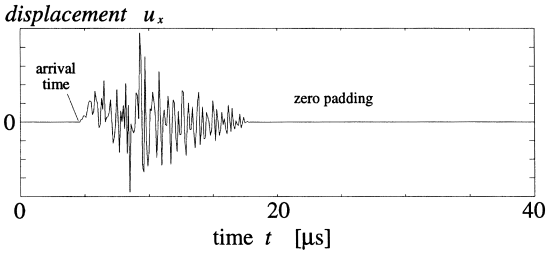

Fig. 2. In-plane displacement u_x of a node at upper surface; signal is windowed with a cut-off time of 17 μs.

For this demonstration, only the x displacements at nodes on the upper surface of the plate are considered; only the in-plane displacement results are used for the 2D-FFT. For the sampled data, spatial and temporal aliasing effects have to be avoided. Aliasing is an effect caused by sampling a continuous signal with a digital sampling rate. If the continuous signal contains frequencies above half the sampling rate (Nyquist frequency), the frequency content of the sampled data above the Nyquist frequency is spurious. As a result, the (spatial and temporal) sampling rate for the 2D-FFT must be chosen high enough to avoid aliasing for the frequency and wavenumber range under consideration. Since the upper frequency limit under consideration is 5 MHz, a sampling rate of $\Delta T = 10^{-7}$ s is used. From a FE point of view, the element length $l_e = 0.1$ mm leads to accurate results for $\lambda > \lambda_{min} = 2$ mm [see Eq. (3)]. This results in a maximum value for $1/\lambda = 500\ m^{-1}$. Therefore a spatial sampling step of $\Delta x = 0.5$ mm is used. This means that only solutions of every fifth surface node are needed for the 2D-FFT. The x displacements of 174 surface nodes for 400 time steps form a matrix with 174 columns and 400 rows. The 174 nodes mean that 87 mm of the plate is used for the analysis of the numerical solution. 400 time steps correspond to a total time of 40 μs. In order to get a signal without reflections from the right end of the plate, the time signal is windowed with a cut-off time of 17 μs. This cut-off time corresponds to the time a longitudinal wave needs to travel from one end of the plate to the other. The solution for times larger then 17 μs are ignored and replaced by zero in order to increase the frequency resolution of the time FFT (zero padding), and the 2D-FFT is performed on this matrix. Another way to avoid unwanted reflections is to use new techniques for modelling unbounded media [8] with energy absorbing elements. Unfortunately, such elements are not yet available in ANSYS 5.3 (and in most other general-purpose FE codes), so they are not used in this study.

Fig. 3 shows the $1/\lambda$-f-spectrum, while the contour plot of this spectrum is shown in Fig. 4(a). It can be seen clearly from this figure that only certain $1/\lambda$-f-combinations have meaningful amplitudes; these values are solutions to Eq. (4), the Rayleigh–Lamb equation. Fig. 4(b) shows the magnitude of one column of the spectrum; each peak (marked with an arrow) represents a $1/\lambda$-f-combination that satisfies Eq. (4). Note that there are also some spurious peaks [e.g. left of the second identified peak in Fig. 4(b)] caused by data-sampling and numerical errors. The discrete ''x'' in Fig. 4(a) indicates the location of a peak in a column of the spectrum. The exact solutions of Eq. (4) are plotted as solid lines; there is excellent agreement between the numerical (FE) and analytical (exact) results. For this FE model, the recommended ratio $\lambda/l_e = 20$ is reached for $1/\lambda = 500\ m^{-1}$. The fact that there is good agreement even for higher values of $1/\lambda$ leads to the conclusion that this wavelength limit is not that critical. However, Fig. 4a) shows that the ratio between the integration time step, Δt, and the frequency, f_{max}, is much more critical; the numerical solutions get worse, the closer the ratio $1/(\Delta T\, f_{max})$ gets to the recommended value of 20. In summary, this model of a plate shows that a commercial FE can be used to model the dispersive nature of guided waves.

Next, a more complicated geometry, a steel ring, is

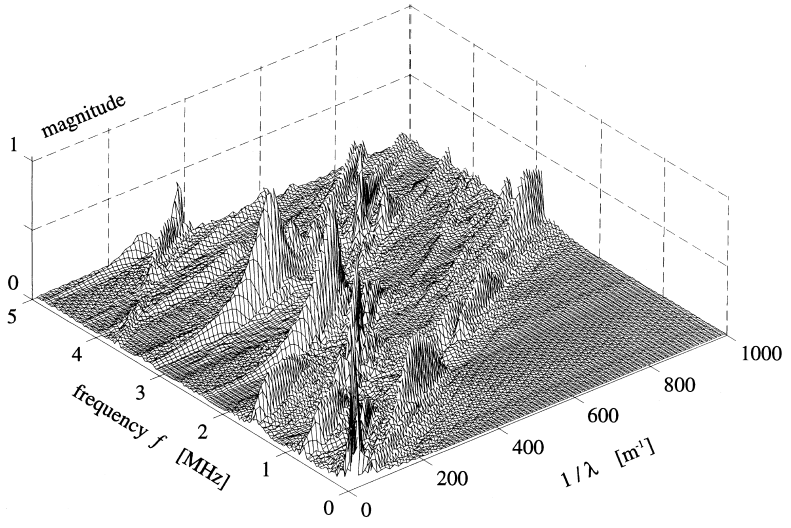

Fig. 3. Spectrum of steel plate obtained by 2D-FFT.

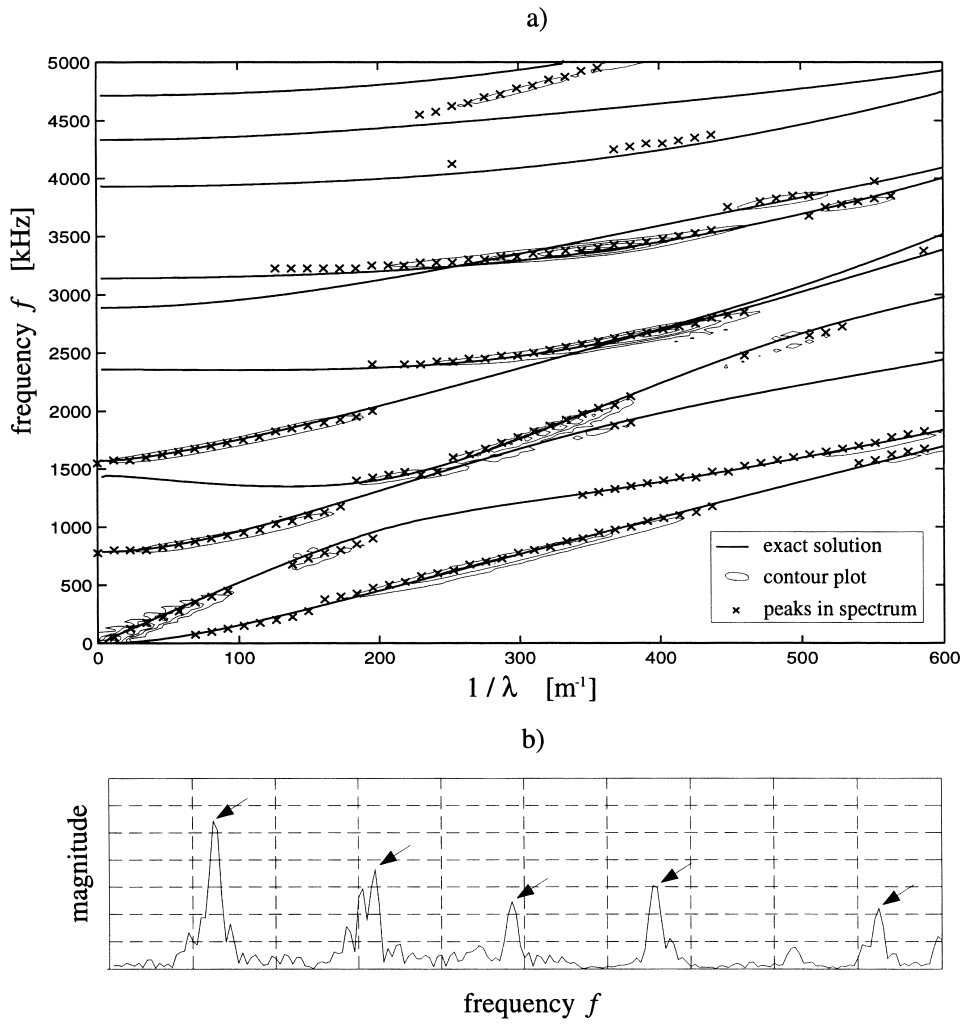

Fig. 4. (a) Frequency spectrum of plate: exact solutions of Rayleigh–Lamb equation and numerical results (contour plot and peaks); (b) magnitude of matrix column obtained by 2D-FFT.

modeled. This problem demonstrates the potential of the FE method to model guided waves in a ''complicated'' structure of realistic size (the travel distance is more than one order of magnitude larger than the wavelength). The ring structure under consideration is shown in Fig. 5, and its material properties, steel, are summarized in Table 2 as Material II. The ring is loaded on its outer surface with a point force, $f(t)$, that acts perpendicular to the surface. Due to the fact that the problem is symmetric, only half of the ring needs to be modeled. The boundary conditions are that the nodes in the symmetry plane cannot move in the y-direction. This boundary condition is noted in the right half of Fig. 5 by rollers. The time function of the input load, $f(t)$, and its frequency content are given in Fig. 6. This frequency content supposes that frequencies above 1 MHz are not of interest.

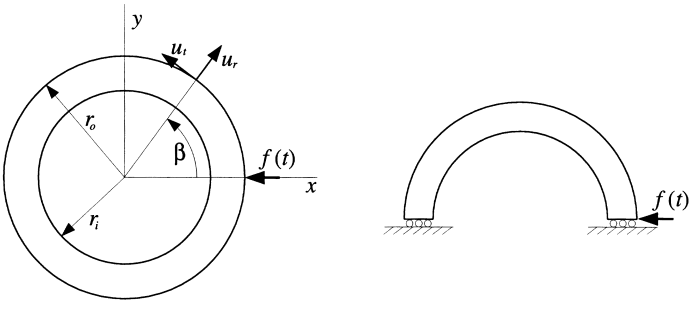

Fig. 5. Symmetric problem: ring loaded with point force $f(t)$.

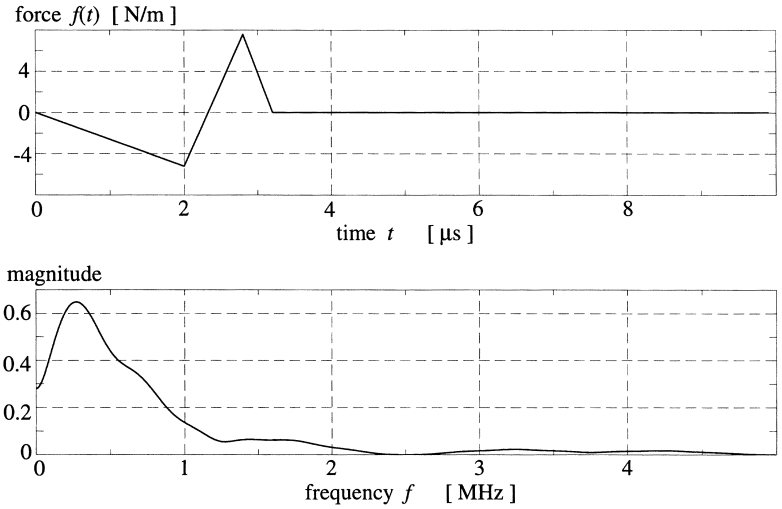

Fig. 6. Time function and frequency content of the concentrated load $f(t)$.

Table 3
Integration time steps, needed calculation times and frequency limits for model II and real time of 55 μs

Integration time step Δt	Calculation time t_{cal}	Frequency limit f_{max}
0.2 μs	8.5 h	0.25 MHz
0.1 μs	17 h	0.5 MHz
0.05 μs	36 h	1.0 MHz
0.025 μs	78 h	2.0 MHz

An optimum FE model of the ring is developed with respect to integration time step, Δt and mesh density; the details of this convergence study are given in Ref. [9]. A description of this ''convergent'' model is shown in Table 1 as Model II, while the corresponding calculation times for real times of 55 μs and the frequency limit calculated with Eq. (2) are given in Table 3. These calculations are done with different Windows NT machines with a Pentium 200 processor and 128 MB RAM.

Using this FE model, the distance between the source and the receiver (measured as angle β) is varied; Fig. 7 shows the wave propagating along the outer surface of the ring. The different plots are the radial surface velocities, $\dot{u}_r$, for

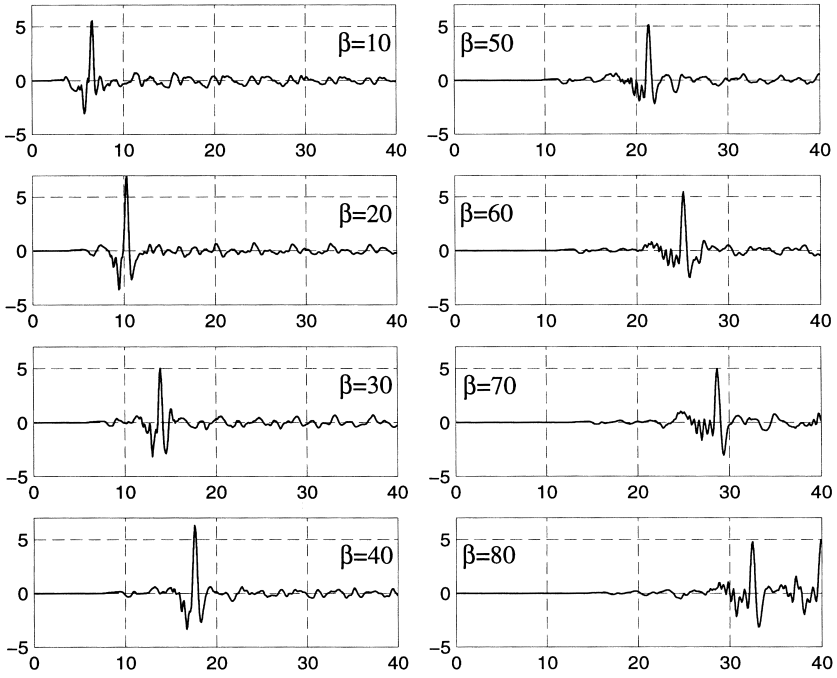

Fig. 7. Surface velocity $\dot{u}_r$ in [10^{-6} m/s] along outer surface for various angles β plotted over time t in [μs].

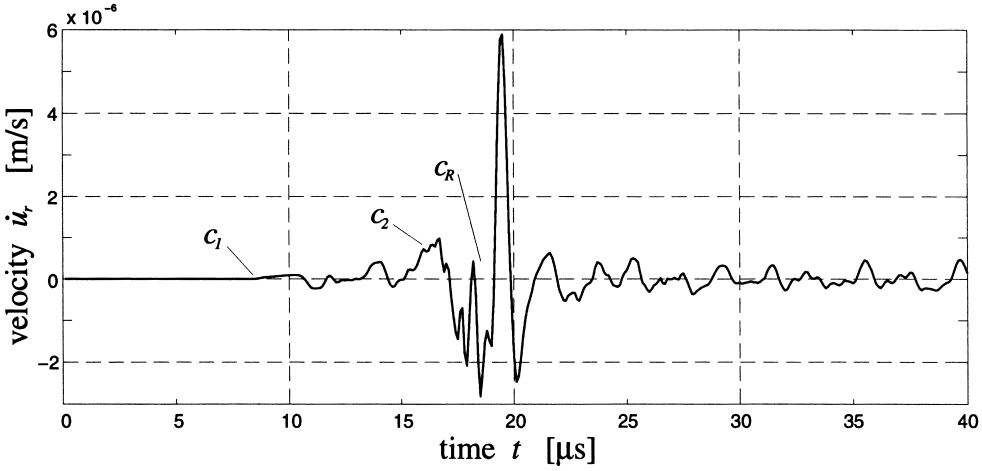

Fig. 8. Identification of the arrival of P, SV and surface waves.

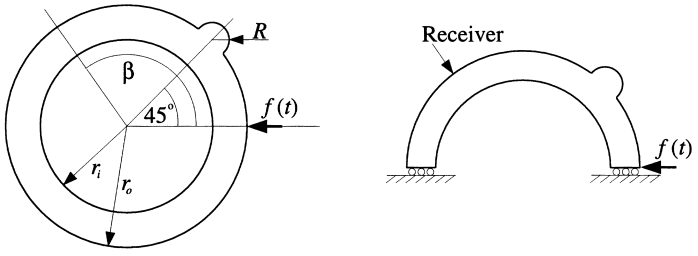

Fig. 9. Modified ring geometry.

different angles, β. The dominant feature in all these plots is the surface wave, the first mode that propagates in the ring. The fact that the shape of this wave changes for increasing angles, β, qualitatively shows that waves in the annular ring are dispersive. The element length, $l_e = 0.3$ mm, of Model II is compared to the wavelength, λ, of the main feature shown in Fig. 7, the surface wave. This surface wave is comparable to the Rayleigh wave on a planar surface although it travels slightly faster than a Rayleigh wave on a flat surface [2, 3]. Using the general correlation between the frequency, the wave speed and the wavelength, $c = \lambda f$, the Rayleigh wave speed $c_R = 2886$ m/s and $f = f_{max} = 1$ MHz as the largest important frequency (from Fig. 6), the smallest wavelength is estimated as $\lambda \approx 2.9$ mm. The ratio between this wavelength and the element length is $\lambda/l_e \approx 10$. Considering that the actual wave speed of the first mode is a little bigger than c_R, and that the important frequencies are smaller than assumed, this ratio might be increased to 15. This value is still below the recommendation $(\lambda/l_e)_{rec} = 20$ given in Eq. (3).

Next, examine the arrival of the different features shown in Fig. 8. This figure shows the radial velocity, $\dot{u}_r$, for $\beta = 45°$. The first time the velocity, $\dot{u}_r$, differs significantly from zero, $t_1 = 8.4$ μs, corresponds to the theoretical arrival time of a longitudinal wave (C_1) propagating directly from the source to the receiver. The theoretical arrival time of the shear wave that travels directly from the source to the receiver is $t_2 = 15.4$ μs (C_2). The theoretical arrival time of the surface wave can be estimated by the Rayleigh surface wave (C_R) on a planar surface and the arc length from the source to the receiver, $t_{R,planar} = 17.2$ μs. The surface wave on a curved surface travels either faster or slower than the Rayleigh surface wave on a planar surface, depending on whether the surface is convex or concave. In Ref. [2], the velocity, c, of such a wave on a convex surface is described with the following equation:

$$c = c_R(1 + \delta), \tag{5}$$

where δ is a small correction factor depending on the material's elastic properties and the wavenumber, ξ, where $\delta \to 0$ as $\xi \to \infty$ and is given in Ref. [2]. This same excellent agreement between theoretical and numerically predicted arrival times is also seen for other receiver positions, β, and demonstrates the accuracy of the FE solution.

Finally, the geometry of the ring is modified slightly to demonstrate the robustness of the FE method. In an analytical solution, a slight change in geometry can cause major solution difficulties, but the FE method can model these more realistic shapes without any additional complications. For example, the geometry of the ring is modified as shown in Fig. 9. Two different sized ''perturbations'' (semi-circular areas) are added to the ideal ring. The radii of these semi-circular areas are $R = 5$ and 10 mm. For comparison purposes, the ideal ring is presented as well. Fig. 10 shows the radial velocity $\dot{u}_r$, for the various cases with an angle $\beta = 112.5°$. The main feature of the ideal ring, the

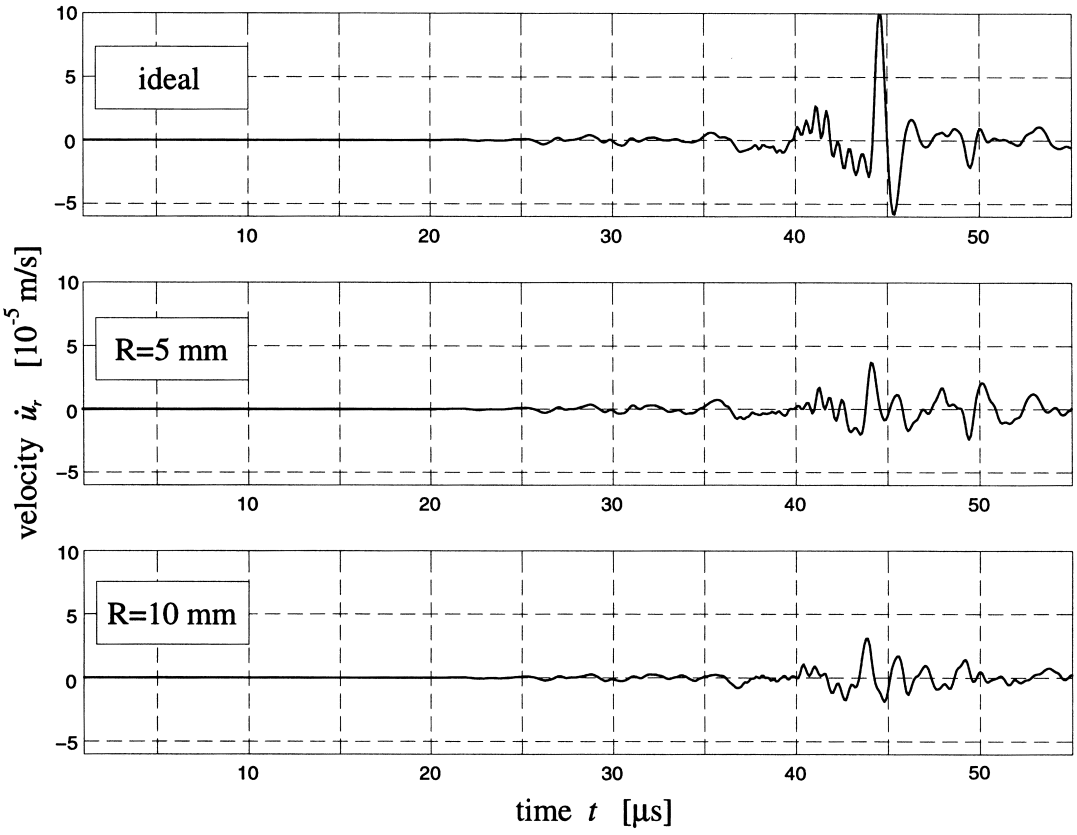

Fig. 10. Comparison of modified ring geometries: radial velocity $\dot{u}_r$ for $\beta = 112.5°$.

surface wave, disappears in the two other cases. This leads to the conclusion that the first mode is tied to the convex surface and if this geometry is disturbed, this mode can no longer propagate.

4. Comparison with other approaches

The FE results (Model II and Material II) are first compared with an analytical solution using the mode superposition method [3]. Briefly, the first step for the mode superposition method is to explicitly solve the eigenvalue problem for the set of ring dimensions. Next, the transient problem for the load shown in Fig. 6 is solved by mode expansion [3]. The radial displacements, u_r, at a 90° angle between the source and the receiver are plotted in Fig. 11 and compared with the FE results. The excellent agreement between these two solutions illustrates that the FE method does an outstanding job in modeling wave propagation problems in wave guides. It also confirms that the FE solution converges toward the correct value using parameters chosen according to Eqs. (2) and (3).

As another benchmark, these FE results are compared with experimentally obtained waveforms. Optical generation and detection of ultrasonic waves [10] is used in these experiments, which comes very close to the ideal case of a point source and receiver assumed with the FE method. The main difference between the FE model and the experimental procedure is that the frequency content of the experimental source is broad band, while the numerical source has a limited frequency content. However, both sources mainly excite the first mode, the surface wave propagating along the outer surface. Since this mode propagates in an almost non-dispersive fashion, its arrival time is nearly frequency independent and can be used to compare the experimental and FE results. The arrival time of the main peak of the first mode is measured (numerically and experimentally) for different travel distances between source and receiver. Fig. 12 shows experimental results for different travel distances (indicated by angle β); these plots correspond to the FE results in Fig. 7. The numerical peaks arrive 1.7%–4.2% earlier than the experimentally measured peaks. This difference can be explained by the slightly decreasing phase velocity of the first mode with increasing frequency; the early arrival makes sense, and provides another demonstration of the accuracy of the FE method.

5. Conclusion

This research clearly illustrates the effectiveness of using the FE method to model 2D guided wave propagation problems, specifically demonstrating the potential of the FE method for problems when an analytical solution is

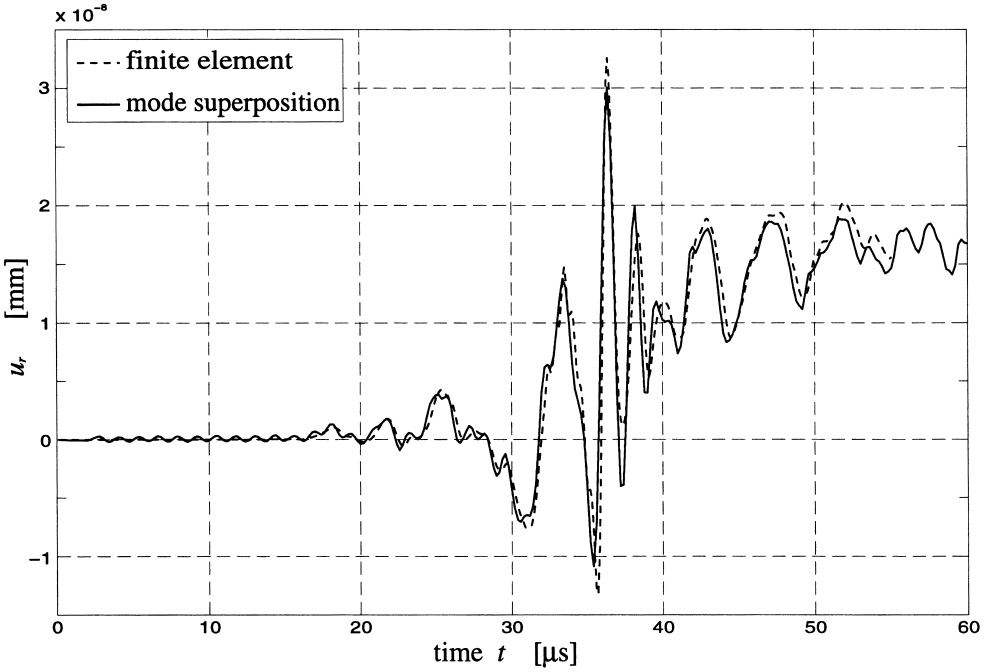

Fig. 11. Comparison of the mode superposition and the FE solution.

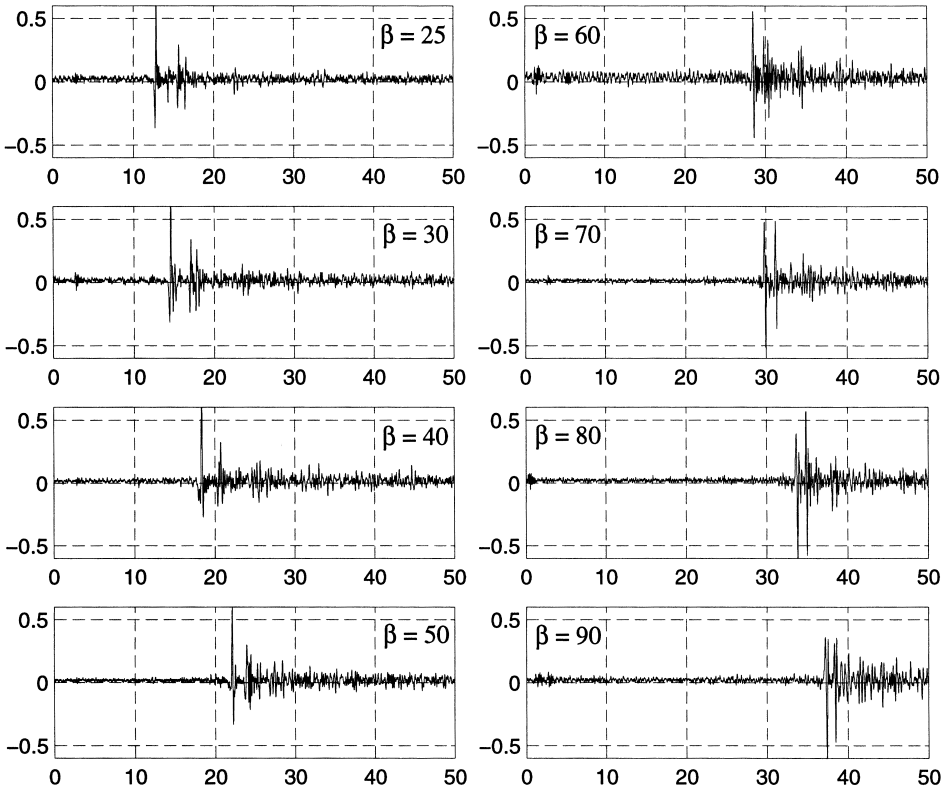

Fig. 12. Experimentally obtained (normalized) radial velocities v_r for various angles β, time t in [μs].

not possible because of a ''complicated'' component geometry. This research establishes the foundation mechanics to numerically solve guided wave propagation in complex structures and uses the powerful post-processing capabilities of a commercial FE code to study and interpret guided wave propagation phenomena.

An investigation into the influence of the two most important FE parameters, the mesh density (element length) and

the time step size between solution points (integration time step), is completed by first studying a problem where a well established analytical solution is available, a flat plate. The FE solution converges for certain values of element length and integration time step, so that an optimized model is developed. This optimization is critical in order to avoid unnecessarily high hardware requirements and enormous total calculation times. The optimized FE parameters are related to wave propagation attributes in order to establish benchmark criteria, and the correlation between these parameters is discussed. For example, the highest wave frequency affects the integration time step while the shortest wavelength influences the element length. The numerical results are in complete agreement with the analytical solution; both models illustrate the geometric dispersion that is present in a wave guide.

The experience gained in the flat plate example is next applied to an annular ring. By using these optimized parameters, different wave propagation phenomena in an ideal ring are investigated. For example, arrival times of waves propagating directly between two points are compared to theoretical values; arrival times of numerical wave features are correlated with experimental results; and the FE results are directly compared to an analytical solution. All these comparisons confirm the high accuracy of FE solutions when applied to wave propagation problems.

In order to show the real advantage of the FE method over analytical solutions, the geometry of the ring is slightly changed. It is in these types of examples that the FE method exhibits its advantages over analytical approaches; the FE method (can potentially) provide a solution for any geometry, as long as this geometry and its boundary conditions can be modeled. However, some special steps, like mesh refining at anticipated stress concentrations, may be necessary. An additional advantage of the FE model is that the numerical results can be elegantly presented using the post-processing, graphical capabilities inherent to the program. For example, a snapshot of the displacement field or a color plot of the stress distributions can give new insights into wave propagation phenomena.

Acknowledgements

This work is partially supported by the DAAD (Deutscher Akademischer Austausch Dienst) and by the Office of Naval Research M-URI program ‘‘Integrated Diagnostics’’ (grant number: N000014-95-1-0539). We would also like to thank the technical support group of Swanson Analysis Systems Inc.

References

[1] Graff KF. Wave motion in elastic solids. New York: Dover, 1975.
[2] Viktorov IA. Rayleigh and lamb waves: physical theory and application. Moscow: Acoustics Institute, Academy of Science of the USSR, 1967 (translated from Russian by Warren P. Mason).
[3] Liu G, Qu J. Transient wave propagation in a circular annulus subjected to impulse excitation on its outer surface. J Acoust Soc Am 1998; (in press).
[4] Alleyne D, Cawley P. A two-dimensional Fourier transform method for measurement of propagating multimode signals. J Acoust Soc Am 1991;89(3):1159–68.
[5] Bathe K-J. Finite element procedures. Englewood Cliffs, NJ: Prentice Hall, 1996.
[6] ANSYS user’s manual for revision 5.0. Houston, TX: Swanson Analysis Systems, 1992.
[7] Costley RD, Berthelot YH, Jacobs LJ. Fresnel arrays for the study of Lamb waves in laser ultrasonics. J Nondestruct Eval 1994;13(1):33–42.
[8] Wolf JP, Song C. Finite element modelling of unbounded media. New York: Wiley, 1996.
[9] Moser F. Application of finite element methods to study transient wave propagation in elastic wave guides. Diplomarbeit Thesis, Institute A of Mechanics, University of Stuttgart, 1997.
[10] Bruttomesso DA, Jacobs LJ, Fiedler C. Experimental and numerical investigation of the interaction of Rayleigh surface waves with corners. J Nondestruct Eval 1997;16(1):21–30.